Flatness-based feed-forward control of an HVDC power transmission network

C. Schmuck
Max-Planck-Institute for Dynamics of Complex Technical Systems,
39106 Magdeburg, Germany
e-mail: schmuck@mpi-magdeburg.mpg.de

F. Woittennek
Institut für Regelungs- und Steuerungstheorie,
Technische Universität Dresden,
01062 Dresden, Germany
e-mail: frank.woittennek@tu-dresden.de

A. Gensior
Elektrotechnisches Institut,
Technische Universität Dresden
01062 Dresden, Germany
e-mail: albrecht.gensior@tu-dresden.de

J. Rudolph
Lehrstuhl für Systemtheorie und Regelungstechnik,
Universität des Saarlandes,
66041 Saarbrücken, Germany
e-mail: j.rudolph@lsr.uni-saarland.de

Abstract—**An efficient and well-established technology for power transmission across long distances is high voltage direct current transmission (HVDC). However, HVDC is up to now almost completely limited to peer-to-peer connections or networks with peers situated closely to each other. This contribution introduces the flatness-based design of a feedforward control of tree-like, i.e. cycle-free, HVDC transmission networks comprising two or more converter stations. The resulting control concept allows a flexible determination of the power distribution within the network. Furthermore, effects like power losses and delays due to wave propagation, which are related especially to long transmission lines, can be easily taken into account. Numerical simulations for an example network are included to prove the value of the results.**

Power grid; Multi-Terminal HVDC; Travelling waves on transmission lines; Flatness-based control;

I. INTRODUCTION

Electric power transmission by means of alternating current (AC) is not feasible for transmission distances larger than 1000 km due to high reactive currents and undesired wave reflections. High voltage direct current transmission (HVDC) is an efficient alternative to overcome these limitations [1,2]. The well-established standard configuration of an HVDC system is a peer-to-peer link connecting two conventional AC networks as depicted in Fig. 1. The AC network and the DC link are coupled by a converter terminal equipped with a power converter [3], which works as inverter or rectifier depending on the direction of the power flow.

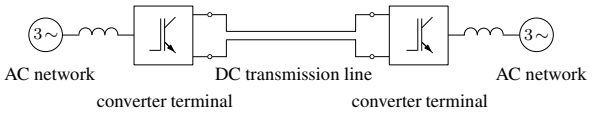

Fig. 1. Peer-to-peer HVDC link with two converter terminals and a DC transmission line connecting them

Although, up to now the vast majority of all implemented HVDC systems are in standard peer-to-peer configuration, there has been increasing interest in HVDC networks with more than two converter terminals, the so called Multi-terminal HVDC [1,4–6]. As a result of the evolving technology for power converters and the increasing exploitation of renewable energy resources such networks have been put into practice, e.g. for offshore wind farms [7–9]. A central goal for the control of an HVDC Multi-Terminal network is to keep the power balance between the electrical power fed into and taken from the DC network by the connected converter stations. At the same time one desires to adjust the power distribution between the converter terminals flexibly during the operation of the system. Furthermore, time delays due to travelling waves can become considerable for long transmission distances [6] and should then be taken into account. This work proposes a control method that reaches these goals taking a flatness-based approach. For the discussed transmission system, the description of which involves partial differential equations (PDEs), this means that the solution of the system equations is parametrized by the trajectories of a special set of system variables, called a flat output of the system [10–12]. The number of the components of the flat output equals the number of the control inputs.

The remaining part of the paper is structured as follows. Section II describes the mathematical model of the HVDC transmission network. Thereafter, a flat output of this model is derived and the flatness-based control design is explained in section III. The results are illustrated by the numerical example of section IV. Finally, section V gives some remarks on practical issues and on potential extensions to be considered in future work.

II. MODEL OF THE HVDC NETWORK

This section introduces the mathematical model of the HVDC network, which the control design is based on.

A. General network structure

A general transmission network is assumed to consist of n_P uniquely numbered nodes P_μ, $\mu \in \mathcal{P}$ where $\mathcal{P}$ is the set of all node indices existing in the network. Two arbitrary nodes P_μ and P_ν can be connected by an electric transmission line denoted by L_μ^ν where the notations L_μ^ν and L_ν^μ coincide, see Fig. 2. Then $\mathcal{L}$ is the set of the index pairs of all n_L existing lines. Regarding the transmission line L_μ^ν the notation z_μ^ν is used for the spatial coordinate at node P_μ and z_ν^μ is used at node P_ν respectively.

Every node P_μ, $\mu \in \mathcal{P}$ can be connected to a converter terminal which is called C_μ in this case. The set $\mathcal{P}_a \subseteq \mathcal{P}$ comprises the indices of all network nodes equipped with a converter terminal, called active nodes, whereas $\mathcal{P}_p = \mathcal{P} \setminus \mathcal{P}_a$ comprises the indices of all nodes without converter terminal, called passive nodes. Every node which is connected to only one line is called terminating node. Obviously, a passive terminating node would be useless in practice, which is why all terminating nodes are assumed to be active.

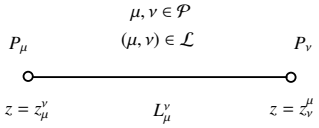

Fig. 2. Notation for nodes and transmission lines in a general network

A node P_μ is called neighbor of node P_ν if there exists a line L_μ^ν, $(\mu, \nu) \in \mathcal{L}$ connecting them. The indices of all m_ν neigbors of P_ν form the set $\mathcal{N}_\nu$.

B. Tree-like networks

The considerations in this paper are restricted to the special case of tree-like, i.e. cycle-free, networks sketched in Fig. 3. The abscence of transmission line cycles implies that the path

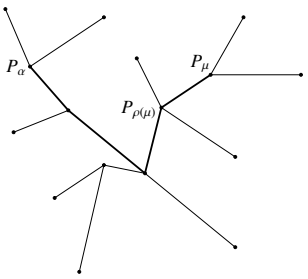

Fig. 3. Network in tree-like structure with an arbitrarily chosen initial node P_α, one of the remaining nodes P_μ and the path between them

between any two converter terminals through the network is unique. Because of this property every node in a circuit-free network has a unique predecessor with respect to a certain initial node. Chosing an arbitrary node $P_\alpha, \alpha \in \mathcal{P}$ as this initial node, the predecessor $P_{\rho(\mu)}$ of $P_\mu, \mu \in \mathcal{P} \setminus \{\alpha\}$ is definded as the node which precedes P_μ on the unique path from P_α to P_μ. Note that the predecessor index $\rho(\mu)$ belonging to node P_μ depends on the choice of the initial node P_α although this is not represented by the notation for the sake of simplicity.

In the case of tree-like networks the notation for transmission lines and their node coordinates may be simplified to

$$L_\mu := L_{\rho(\mu)}^\mu = L_\mu^{\rho(\mu)}, \quad z_{\rho(\mu)}^\mu = 0, \quad z_\mu^{\rho(\mu)} = \ell_\mu,$$

$\forall \mu \in \mathcal{P} \setminus \{\alpha\}$, where ℓ_μ is the length of L_μ. This notation illustrated in Fig. 4 will be used throughout the remaining parts of this work.

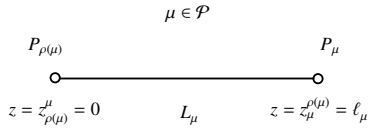

Fig. 4. Simplified notation for nodes and transmission lines in tree-like networks

C. Converter terminals

For each converter terminal C_μ, $\forall \mu \in \mathcal{P}_a$ the voltage is U_μ and the current is I_μ. Thanks to modern semiconductor technology recent power converters allow to generate almost arbitrary current or voltage trajectories at their DC side [3]. Hence, each converter can be seen either as an ideal current source with a freely adjustable current $I_\mu(t)$ or as an ideal voltage source with a freely adjustable voltage $U_\mu(t)$. The AC part of the converter is therefore neglected. The converters are the actuators of the transmission system. If C_μ is chosen to be a current source then I_μ is a control input of the network. Otherwise, if C_μ is chosen to be a voltage source then U_μ is a control input. The control design is independent from this choice which thus can be made according to technical aspects.

D. Transmission line equations and boundary conditions for tree-like networks

The model of the transmission lines should allow to take effects like wave propagation, related delays and transmission losses into account. Therefore, the voltage profile u_μ and the current profile i_μ on each transmission line L_μ, $\mu \in \mathcal{P} \setminus \{\alpha\}$ are described by the hyperbolic system of PDEs

$$\frac{\partial u_\mu}{\partial z}(z,t) + L\frac{\partial i_\mu}{\partial t}(z,t) + R i_\mu(z,t) = 0 \tag{1a}$$

$$\frac{\partial i_\mu}{\partial z}(z,t) + C\frac{\partial u_\mu}{\partial t}(z,t) + G u_\mu(z,t) = 0 \tag{1b}$$

with $z \in (0, \ell_\mu)$, $t > 0$ and the constant positive, line-specific parameters R, G, L and C [13]. The current i_μ is considered positive in the direction assigned to line L_μ which is from $P_{\rho(\mu)}$ to P_μ.

The electrical interconnection of the transmission lines at the network nodes leads to a coupling of the corresponding line PDEs at their boundaries, see Fig. 5 and Fig. 6. The boundary conditions at each node P_μ result from Kirchhoff's current and voltage laws. The current law yields

$$-\sum_{k \in \mathcal{N}_\alpha} i_k(0,t) = \begin{cases} I_\alpha(t), & \text{if } \alpha \in \mathcal{P}_a \\ 0, & \text{if } \alpha \in \mathcal{P}_p \end{cases} \tag{2a}$$

for the boundary values of the line currents at the initial node P_α and

$$i_\mu(\ell_\mu, t) - \sum_{\substack{k \in \mathcal{N}_\mu \\ k \neq \rho(\mu)}} i_k(0,t) = \begin{cases} I_\mu(t), & \forall \mu \in \mathcal{P}_a \setminus \{\alpha\} \\ 0, & \forall \mu \in \mathcal{P}_p \setminus \{\alpha\} \end{cases} \tag{2b}$$

for the remaining nodes. The converter current $I_\mu(t)$ is defined to be positive if it is directed away from node P_μ. Kirchhoff's voltage law leads to

$$u_k(0,t) = \bar{u}_\mu(t), \quad \forall k \in \mathcal{N}_\mu \setminus \{\rho(\mu)\}, \quad \forall \mu \in \mathcal{P} \tag{3a}$$

$$u_\mu(\ell_\mu, t) = \bar{u}_\mu(t), \quad \forall \mu \in \mathcal{P} \setminus \{\alpha\} \tag{3b}$$

for the boundary values of the line voltages at P_μ with $\bar{u}_\mu(t)$ denoting the node voltage at P_μ. Accordingly, the voltages at the converters connected to the active nodes of the network are

$$U_\mu(t) = \bar{u}_\mu(t), \quad \forall \mu \in \mathcal{P}_a. \tag{3c}$$

Altogether, the $2n_L$ PDEs (1) and the boundary conditions (2) and (3) constitute a linear distributed parameter model of the transmission network. The currents I_μ or the voltages U_μ, $\mu \in \mathcal{P}_a$ of the converter terminals are the concentrated control inputs located at the boundaries of the transmission lines.

III. FLATNESS-BASED CONTROL DESIGN

This section deals with the design of a flatness-based feedforward control for the transmission network model described in section II. It is shown that the trajectories of all system variables can be calculated from prescribed trajectories of the current I_α and the voltage U_α of the converter at an arbitrarily chosen initial node P_α and some current allocation parameters (CAP), which are introduced additionally at each network node. Therefore, the mentioned variables form a flat output of the system. Once the trajectories for the flat output are chosen the remaining system trajectories can be conveniently calculated from node to node. Finally, this yields the desired control input trajectories for the converter currents or voltages.

A. Derivation of a flat output

Initial node The first step is to choose an arbitrary node with converter terminal as the initial node P_α, $\alpha \in \mathcal{P}_a$. This determines the simplified notation for the network, which is clarified by Fig. 5 and Fig. 6. In the following the system variables shall be calculated from some prescribed current $I_\alpha(t)$ and voltage $U_\alpha(t)$ at C_α. Because of (3a) and (3c), the converter voltage U_α directly gives the line voltages

$$u_k(0,t) = U_\alpha(t), \quad \forall k \in \mathcal{N}_\alpha \tag{4}$$

of the lines connected at P_α. In order to determine the currents at P_α one introduces m_α real, time-varying current allocation parameters (CAP) σ_α^k, $\forall k \in \mathcal{N}_\alpha$, such that

$$i_k(0,t) = -\sigma_\alpha^k(t) I_\alpha(t), \quad \forall k \in \mathcal{N}_\alpha, \tag{5}$$

where

$$\sum_{k\in\mathcal{N}_\alpha} \sigma_\alpha^k(t) = 1 \tag{6}$$

has to be guaranteed to avoid the violation of the current law (2a). This means that the trajectories for $(m_\alpha - 1)$ of the m_α new parameters can be chosen freely to determine the desired fraction (5) of $I_\alpha(t)$ for each line L_k, $\forall k \in \mathcal{N}_\alpha$ at node P_α. The vector comprising these $(m_\alpha - 1)$ chosen parameters as components is denoted by $\boldsymbol{\sigma}_\alpha$ in the following. The equations (4)–(6) give a complete parametrization of the line voltages $u_k(0,t)$ and currents $i_k(0,t), \forall k \in \mathcal{N}_\alpha$ at node P_α in terms of U_α, I_α and $\boldsymbol{\sigma}_\alpha$.

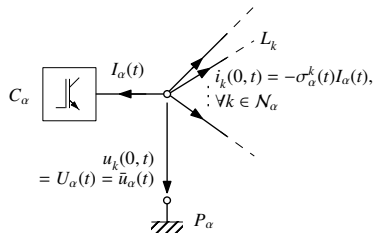

Fig. 5. Currents and voltages at the initial node P_α, $\alpha \in \mathcal{P}_a$

Remaining nodes Fig. 6 shows one of the remaining network nodes P_μ, $\mu \in \mathcal{P} \setminus \{\alpha\}$, its unique predecessor $P_{\rho(\mu)}$ and the line L_μ connecting them. The solution of the line equations (1) allows for the direct calculation of the voltage and current trajectories of line L_μ at P_μ from some known voltage and current trajectories at the preceeding end at $P_{\rho(\mu)}$ by

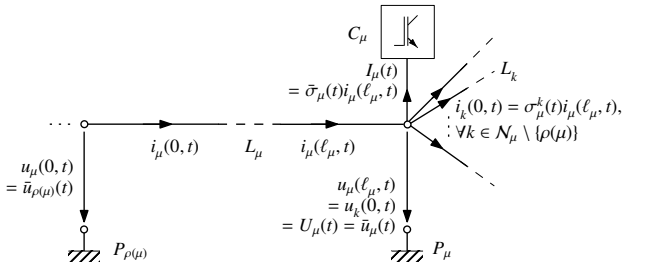

Fig. 6. Currents and voltages at one of the remaining nodes P_μ, $\mu \in \mathcal{P}_a \setminus \{\alpha\}$ and the connected line L_μ

$$\begin{aligned} u_\mu(\ell_\mu, t) = {} & \frac{e^{-\gamma\tau_\mu}}{2} u_\mu(0, t-\tau_\mu) + \frac{e^{\gamma\tau_\mu}}{2} u_\mu(0, t+\tau_\mu) \\ & + \int_{-\tau_\mu}^{\tau_\mu} g(\ell_\mu, \bar{t})\, u_\mu(0, t-\bar{t})\, \mathrm{d}\bar{t} \\ & + \sqrt{\frac{L}{C}} \left(\frac{e^{-\gamma\tau_\mu}}{2} i_\mu(0, t-\tau_\mu) - \frac{e^{\gamma\tau_\mu}}{2} i_\mu(0, t+\tau_\mu) \right) \\ & - \int_{-\tau_\mu}^{\tau_\mu} h_u(\ell_\mu, \bar{t})\, i_\mu(0, t-\bar{t})\, \mathrm{d}\bar{t}, \end{aligned} \tag{7a}$$

$$\begin{aligned} i_\mu(\ell_\mu, t) = {} & \frac{e^{-\gamma\tau_\mu}}{2} i_\mu(0, t-\tau_\mu) + \frac{e^{\gamma\tau_\mu}}{2} i_\mu(0, t+\tau_\mu) \\ & + \int_{-\tau_\mu}^{\tau_\mu} g(\ell_\mu, \bar{t})\, i_\mu(0, t-\bar{t})\, \mathrm{d}\bar{t} \\ & + \sqrt{\frac{C}{L}} \left(\frac{e^{-\gamma\tau_\mu}}{2} u_\mu(0, t-\tau_\mu) - \frac{e^{\gamma\tau_\mu}}{2} u_\mu(0, t+\tau_\mu) \right) \\ & - \int_{-\tau_\mu}^{\tau_\mu} h_i(\ell_\mu, \bar{t})\, u_\mu(0, t-\bar{t})\, \mathrm{d}\bar{t} \end{aligned} \tag{7b}$$

with $\tau_\mu = \sqrt{LC}\ell_\mu$ and the functions

$$\begin{aligned} h_u(z,t) &= Rf(z,t) + L\frac{\partial f}{\partial t}(z,t), \\ h_i(z,t) &= Gf(z,t) + C\frac{\partial f}{\partial t}(z,t), \\ g(z,t) = \frac{\partial f}{\partial z}(z,t), \quad & f(z,t) = \frac{e^{-\gamma t}}{2\sqrt{LC}} J_0(\beta\sqrt{LCz^2 - t^2}) \end{aligned}$$

employing the bessel function J_0 of the first kind and the constants

$$\beta = \frac{1}{2}\left(\frac{R}{L} - \frac{G}{C}\right), \quad \gamma = \frac{1}{2}\left(\frac{R}{L} + \frac{G}{C}\right),$$

see [14]. Equations (7) reflect the wave propagation process taking place on line L_μ, since they involve distributed delays and predictions. This means the values $u_\mu(\ell_\mu, t)$ and $i_\mu(\ell_\mu, t)$ at a certain time instant t are determined by the trajectories of $u_\mu(0, \bar{t})$ and $i_\mu(0, \bar{t})$ on the complete time intervall $\bar{t} \in [t - \tau_\mu, t + \tau_\mu]$. The delay τ_μ can be interpreted as the time that a voltage and current wave needs to travel between the ends of L_μ.

Analogously to the procedure at the initial node the distribution of the currents between the lines and a possibly connected converter at P_μ shall be determined by $(m_\mu - 1)$ CAPs σ_μ^k, $\forall k \in \mathcal{N}_\mu \setminus \{\rho(\mu)\}$ and an additional CAP $\bar{\sigma}_\mu$ if P_μ is active. This means

$$i_k(0,t) = \sigma_\mu^k(t)\, i_\mu(\ell_\mu, t), \quad \forall k \in \mathcal{N}_\mu \setminus \{\rho(\mu)\} \tag{8a}$$

$$I_\mu(t) = \bar{\sigma}_\mu(t)\, i_\mu(\ell_\mu, t), \quad \text{if } \mu \in \mathcal{P}_a. \tag{8b}$$

Again Kirchoff's current law (2b) requires

$$\sum_{\substack{k \in \mathcal{N}_\mu \\ k \neq \rho(\mu)}} \sigma_\mu^k(t) = \begin{cases} 1, & \text{if } \mu \in \mathcal{P}_p \\ 1 - \bar{\sigma}_\mu(t), & \text{if } \mu \in \mathcal{P}_a. \end{cases} \tag{9}$$

Due to (9) one can freely chose the trajectories for only $(m_\mu - 2)$ out of $(m_\mu - 1)$ CAPs if $\mu \in \mathcal{P}_p$ or $(m_\mu - 1)$ out of m_μ CAPs if $\mu \in \mathcal{P}_a$. The vector comprising these chosen parameters as components is denoted by $\boldsymbol{\sigma}_\mu$. According to (3) the voltages at P_μ are

$$u_k(0,t) = \bar{u}_\mu(t) = u_\mu(\ell_\mu, t), \quad \forall k \in \mathcal{N}_\mu \setminus \{\rho(\mu)\} \tag{10a}$$

$$U_\mu(t) = u_\mu(\ell_\mu, t), \quad \text{if } \mu \in \mathcal{P}_a. \tag{10b}$$

The equations (7)–(10) give a parametrization of all voltages and currents at P_μ in terms of the voltage $u_\mu(0,t)$ and the current $i_\mu(0,t)$ at the preceeding node $P_{\rho(\mu)}$ and the CAPs $\boldsymbol{\sigma}_\mu$ at P_μ. These equations hold for all remaining nodes P_μ, $\mu \in \mathcal{P} \setminus \{\alpha\}$. Therefore, it is now possible to calculate all voltage and current trajectories at each node in the network from the trajectories of U_α and I_α at the initial node and the freely determined CAP trajectories $\boldsymbol{\sigma}_\mu$, $\forall \mu \in \mathcal{P}$ at the network nodes. Hence, these variables form the flat output

$$\boldsymbol{y} = \left(U_\alpha, I_\alpha, \left(\boldsymbol{\sigma}_\mu\right)_{\forall \mu \in \mathcal{P}}\right) \tag{11}$$

of the transmission network.

Clearly, it is convenient to perform the calculations of the system trajectories stepwise from node to node beginning at the initial node P_α. At first (4) and (5) are used to determine the voltage and current trajectories at node P_α from the determined trajectories of U_α, I_α and the chosen CAPs $\boldsymbol{\sigma}_\alpha$. After that the neighbors of P_α are considered. Their predecessor is P_α. Employing (7)–(10) with $\rho(\mu) = \alpha$ together with the CAP trajectories for each node P_μ, $\mu \in \mathcal{N}_\alpha$ gives all voltage and current trajectories at these nodes. In the next step, these nodes P_μ serve as predecessors for all their neighbors (except P_α) and the equations (7)–(10) can be applied again. One follows this procedure until finally all terminating nodes are reached. A particular result of these calculations are the trajectories of the converter currents I_μ and voltages U_μ, $\mu \in \mathcal{P}_a$ obtained in (8b) and (10b). Together with the trajectories for I_α and U_α these are the feedforward control trajectories that will lead to the system behaviour defined by the previously chosen trajectories for the flat output.

Note that the initial node plays a special role for the operation of the network. In contrast to the other nodes the converter current and voltage trajectories at this node can be chosen freely since they are included in the flat output $\boldsymbol{y}$. Therefore, if a direct determination of the current or voltage trajectories at a certain node is desired for some operational maneuver this node should be chosen as the initial node. It might be useful to choose different initial nodes for different maneuvers. The CAPs being the remaining components of the flat output $\boldsymbol{y}$ determine the current fractions on the transmission lines at each node. This is why they can be used to adjust the power distribution between the converter stations within the network.

B. Trajectory planning: Transition between two states of rest

Several control tasks can be solved much easier if a flat output of the system is known. A particular example is the transition between two states of rest which is relevant for the application of this work, too. Most of the time the HVDC system will be operated in a balanced state of rest with constant voltage and current values which meet all operational requirements. If these requirements change the transition to a suitable new state of rest will be desired.

In a state of rest every system variable remains constant over time by definition. Since for flat systems all trajectories are parametrized by the flat output and its derivatives each state of rest of the system is completely characterized by constant values $\bar{y}_k$ for the n_y components y_k, $k = 1, 2, \ldots, n_y$ of the flat output:

$$y_k(t) = \bar{y}_k, \quad \frac{d^j y_k(t)}{dt^j} = 0, \quad j = 1, 2, \ldots \tag{12}$$

In order to implement the transition from an initial state of rest with $y_k(t) = \bar{y}_k^i$ to a new final state of rest with $y_k(t) = \bar{y}_k^f$ one can chose polynomials $p_k(t)$ to connect the constant parts of the trajectories, such that

$$y_k(t) = \begin{cases} \bar{y}_k^i, & \text{if } t < t_i \\ p_k(t), & \text{if } t_i \leq t \leq t_f \\ \bar{y}_k^f, & \text{if } t > t_f \end{cases} \tag{13}$$

with

$$p_k(t_i) = \bar{y}_k^i, \qquad p_k(t_f) = \bar{y}_k^f, \tag{14a}$$

$$\frac{dp_k}{dt}(t_i) = 0, \qquad \frac{dp_k}{dt}(t_f) = 0, \qquad k = 1, 2, \ldots, n_y. \tag{14b}$$

The obtained trajectory for one component y_k is depicted in Fig. 7. The desired transition time $\Delta t = t_f - t_i$ can be chosen freely.

The conditions (14b) assure continuous differentiability with respect to time for the trajectories of the flat output. This smoothness property is maintained during the computations in section III.A. because derivations with respect to time do not occure. Thus, continuous differentiability is obtained for all system trajectories. The four requirements of (14) can be met with the third order polynomials

$$p_k(t) = \bar{y}_k^i + \left(\bar{y}_k^f - \bar{y}_k^i\right)(3 - 2\bar{t})\,\bar{t}^2, \quad \bar{t} = \frac{t - t_i}{t_f - t_i}, \quad k = 1, 2, \ldots, n_y. \tag{15}$$

The subsequent computation of the remaining system trajectories according to the stepwise procedure of section III comprises the repeated use of (7) including predictions and delays. This entails that the chosen trajectories (13) are involved on some larger time intervall [1] $[t_i - \tau_{\max}, t_f + \tau_{\max}]$ rather that only on $[t_i, t_f]$ as indicated in Fig. 7. The resulting system trajectories and the control input trajectories in particular will leave their initial constant values already up to $\tau_{\max}$ before $t = t_i$ and will reach their final constant values up to $\tau_{\max}$ after $t = t_f$. Again, this reflects the wave propagation process taking place on the transmission lines. In practice this means that an operational maneuver, which intends to change the values of the variables belonging to the flat output $\boldsymbol{y}$ within $t_i \leq t \leq t_f$, has to start at $t = t_i - \tau_{\max}$ and will not end before $t = t_f + \tau_{\max}$.

[1] The maximum delay time $\tau_{\max}$ can be computed by $\tau_{\max} = \max_{k \in \mathcal{P}_t} \tilde{\tau}_k$ where $\mathcal{P}_t$ is the set of the indices of all terminating nodes of the network and $\tilde{\tau}_\mu$ the sum of all delays τ_k of the lines L_k forming the path from the initial node P_α to the terminating node P_μ, $\mu \in \mathcal{P}_t$. This means $\tilde{\tau}_\mu$ is the time that a current and voltage wave needs to travel from the initial node P_α to the terminating node P_μ.

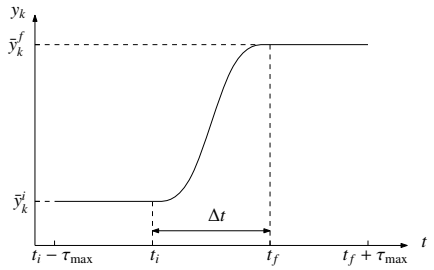

Fig. 7. Polynomial trajectory for one component y_k of the flat output $\boldsymbol{y}$ for the transition between two states of rest

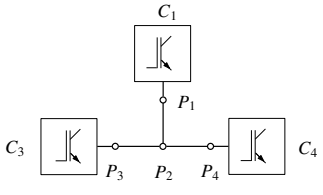

Fig. 8. Example of a circuit-free network with three converters

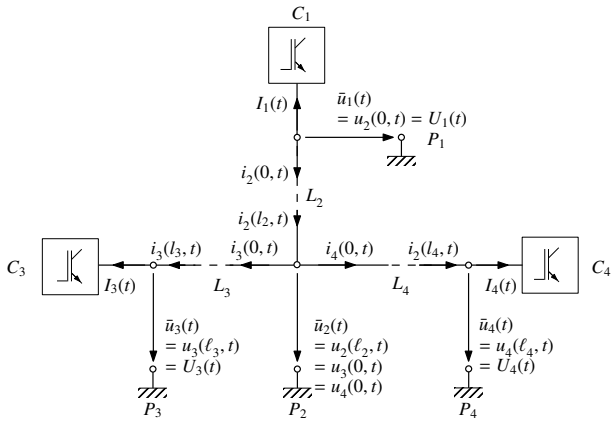

Fig. 9. Circuit-free network with three converters and the notation for the case of P_1 beeing chosen as initial node

IV. A SIMPLE EXAMPLE NETWORK

The results from section III shall now be clarified with the help of a simple example network with $n_P = 4$ nodes and $n_L = 3$ transmission lines shown in Fig. 8. The network is specified by the sets

$$\mathcal{P} = \{1,2,3,4\}, \quad \mathcal{P}_a = \{1,3,4\}, \quad \mathcal{P}_p = \{2\},$$
$$\mathcal{L} = \{(1,2),(2,3),(2,4)\},$$
$$\mathcal{N}_1 = \mathcal{N}_3 = \mathcal{N}_4 = \{2\}, \quad \mathcal{N}_2 = \{1,3,4\}.$$

Hence, the control inputs of the system are the currents or the voltages of the three converters.

It is assumed that the converter current I_1 is required to change from an initial value of 0 to a new constant desired value I_d while the converter voltage U_1 remains at a constant value U_d. Since the voltage and current values at converter C_1 shall be determined node P_1 is chosen as initial node. This yields the notation illustrated in Fig. 9 and the network specific values $\alpha = 1, \rho(2) = 1, \rho(3) = 2$ and $\rho(4) = 2$.

A. Flat output

The stepwise procedure from section III.A. adapts to this example network as follows. According to (11) the first two components of the flat output $\boldsymbol{y}$ are U_1 and I_1. The currents and voltages at P_1

$$u_2(0,t) = U_1(t), \qquad i_2(0,t) = -I_1(t) \tag{16}$$

are obtained using (4) and (5). No CAP is introduced at P_1 because only one transmission line is connected ($m_1 = 1$). Proceeding to the only neighbor of P_1, which is P_2, equations (7) with $\mu = 2$ and $\rho(\mu) = 1$ allow to compute $u_2(\ell_2,t)$, $i_2(\ell_2,t)$ from $u_2(0,t)$, $i_2(0,t)$. Because $m_2 = 3$ lines are connected to the passive node P_2 one needs to introduce $m_2 - 1 = 2$ CAPs σ_2^3, σ_2^4 to determine the currents and voltages

$$u_k(0,t) = u_2(\ell_2,t), \quad i_k(0,t) = \sigma_2^k(t) i_2(\ell_2,t), \quad k = 3,4 \tag{17}$$

according to (8a) and (10a). The trajectory for only $m_2 - 2 = 1$ of the two CAPs σ_2^3, σ_2^4 can be chosen freely. For this example σ_2^3 is selected and is therefore included in the flat output as the third component. After that, the other CAP is determined by (9):

$$\sigma_2^4(t) = 1 - \sigma_2^3(t). \tag{18}$$

Now the last two nodes can be considered. Employing (7) with $\mu = 3, \rho(\mu) = 2$ for line L_3 and again with $\mu = 4, \rho(\mu) = 2$ for line L_4 yields $u_k(\ell_k,t)$, $i_k(\ell_k,t)$, $k = 3,4$. Finally the voltages and currents at the converters C_3 and C_4 follow from (8b):

$$U_k(t) = u_k(\ell_k,t), \qquad I_k(t) = i_k(\ell_k,t) \qquad k = 3,4. \tag{19}$$

At the nodes P_3 and P_4 again no new CAPs are introduced since there is only one line per node ($m_3 = m_4 = 1$). Finally, all system variables are calculated and the flat output of the example network is

$$\boldsymbol{y} = \left(U_1, I_1, \sigma_2^3\right). \tag{20}$$

B. Trajectory planning

Apart from the variables U_1 and I_1 the trajectory for the third component σ_2^3 of $\boldsymbol{y}$ can be prescribed freely as well. It determines how the line current $i_2(\ell_2,t)$ is split between line L_3 and line L_4 and can hence be exploited to set the power distribution between the converters C_3 and C_4. For the sake of simplicity, σ_2^3 shall remain at a constant value of 0.3 during the maneuver to be planned. The two states of rest corresponding to the required current change at C_1 with constant current voltage U_1 and CAP σ_2^3 are characterized by

$$\bar{y}_1^i = U_d, \qquad \bar{y}_2^i = 0, \qquad \bar{y}_3^i = 0.3,$$
$$\bar{y}_1^f = U_d, \qquad \bar{y}_2^f = I_d, \qquad \bar{y}_3^f = 0.3.$$

If the suggested polynomial trajectories (13) with an arbitrarily fixed transition time Δt are now assigned to the variables of the flat output all remaining system trajectories can be computed by the procedure described in section IV.A. In (19) this yields the particularly desired converter current and voltage trajectories. One may chose for each of the three converters either its current or its voltage as control input according to the technical realities of the converter stations. If the calculated converter trajectories are applied to the system it will show the behaviour predefined by the trajectories of the flat output.

To illustrate the results the system trajectories have been computed using a set of numerical parameter values given in TABLE I. The resulting trajectories in Fig. 10 clarify that the transition of the complete system between the two states of rest takes longer than only the prescribed transition time $\Delta t = 5$ ms. The maneuver, which was planned to change I_1 within $t_i \le t \le t_f$, is required to start already at $t = t_i - \tau_{\max} = -20.76$ ms

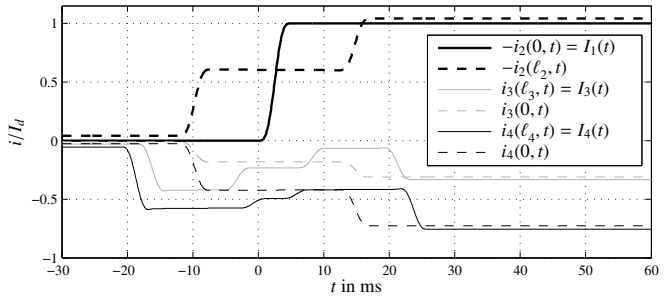

(a) *Currents at the active nodes (solid) and line currents at P_2 (dashed)*

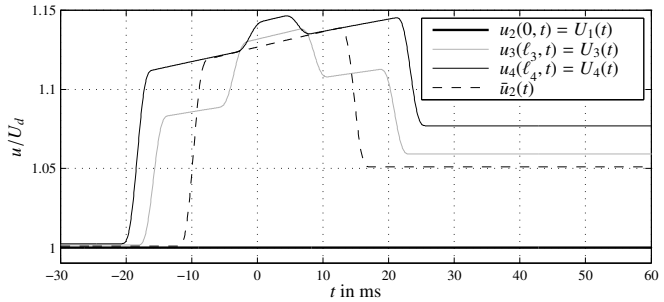

(b) *Voltages at the active nodes (solid) and node voltage at P_2 (dashed)*

Fig. 10. Current and voltage trajectories for the three lines and converters during the transition between two states of rest for a change of the converter current I_1 at converter C_1 from the initial value $\bar{y}_2^i = 0$ to $\bar{y}_2^f = I_d$ via a polynomial trajectory on $0 \le t \le \Delta t = 5ms$

at converter C_4 and ends not before $t = t_f + \tau_{\max} = 25.76$ ms at C_4.[2] The impact of the CAP σ_2^3 is clarified by the dashed graphs in Fig. 10(a). It can be seen that the currents $i_3(0,t)$ and $i_4(0,t)$ are proportional to $i_2(\ell_2,t)$ according to the prescribed constant value $\sigma_2^3(t) = 0.3$.

TABLE I. Numerical parameter values

Parameter	Value	Parameter	Value
R	$1 \cdot 10^{-5}$ Ωm^{-1}	$\tau_2 = \sqrt{LC}\ell_2$	12.25 ms
G	$3 \cdot 10^{-10}$ Sm^{-1}	$\tau_3 = \sqrt{LC}\ell_3$	6.12 ms
L	$5 \cdot 10^{-7}$ Hm^{-1}	$\tau_4 = \sqrt{LC}\ell_4$	8.51 ms
C	$2 \cdot 10^{-10}$ Fm^{-1}	$\tau_{\max} = \tau_2 + \tau_4$	20.76 ms
ℓ_2	1000 km	t_i	0 ms
ℓ_3	500 km	Δt	5 ms
ℓ_4	700 km	$t_f = t_i + \Delta t$	5 ms

V. FURTHER REMARKS AND FUTURE WORK

If an initial node and a certain trajectory form, e.g. (13), is fixed the resulting system trajectories for different trajectory planning procedures will differ only in a few parameters but not in their form. Thus, the complete calculations of section III.A. need to be performed only once for the first planning procedure. For following maneuvers only the trajectory parameters have to be updated. This reduces the computational effort rapidly.

The control scheme suggested in this contribution is particularly useful for HVDC networks with long tranmission lines since wave propagation processes and related delays are taken into account. However, it can be also applied to systems with transmission lines short enough to neglect delays. In this case L and C are set to zero in the line equations (1) which changes them to ordinary differential equations in z. Their solution

$$u_\mu(\ell_\mu,t) = A_{11}^\mu u_\mu(0,t) + A_{12}^\mu i_\mu(0,t) \tag{21a}$$

$$i_\mu(\ell_\mu,t) = A_{21}^\mu u_\mu(0,t) + A_{22}^\mu i_\mu(0,t) \tag{21b}$$

with $A_{11}^\mu = A_{22}^\mu = \cosh(\sqrt{RG}\ell_\mu)$, $A_{12}^\mu = \sqrt{R/G}\sinh(\sqrt{RG}\ell_\mu)$ and $A_{21}^\mu = (G/R)A_{12}^\mu$ replaces (7) in the calculation procedure of section III.A. Because the changed line equations do not model wave propagation anymore no delays and predictions occure in (21). As a result, the duration of a planned meneuver will reduce to Δt.

To face the problem of model uncertainties and disturbances the feed-forward control scheme could be extended by local feed-back controllers at each converter. This is a potential topic for future work.

[2] The maximum delay time $\tau_{\max}$ given in TABLE I is the maximum of the two sums $\tau_2 + \tau_3$ and $\tau_2 + \tau_4$, which refer to the travel time of a voltage and current wave from P_1 to P_3 and to P_4 respectively.

REFERENCES

[1] J. Arrillaga. *High Voltage Direct Current Transmission*, volume 29 of *Power and Energy Series*. The Institution of Electrical Engineers, 1998.

[2] E. Peschke and R. v. Olshausen. *Kabelanlagen für Hoch- und Höchstspannung*. Publicis-MCD-Verlag, 1998.

[3] N. Mohan, T.M. Undeland, and W.P. Robbins. *Power Electronics*. Wiley & Sons., 2002.

[4] P. Karlson. *DC Distributed Power Systems - Analysis, Design and Control for a Renewable Energy System*. PhD thesis, Lund University, 2002.

[5] H. Jiang and A. Ekstrom. Multiterminal HVDC systems in urban areas of large cities. *IEEE Trans. Power Delivery*, 13:1278–1284, 1998.

[6] V.F. Lescale, A. Kumar, L.-E. Juhlin, H. Bjorklund, and K. Nyberg. Challenges with multi-terminal UHVDC transmissions. In *Joint International Conference on Power System Technology and IEEE Power India Conference, POWERCON*, pages 1–7, Oct. 2008.

[7] L. Jun, O. Gomis-Bellmunt, J. Ekanayake, and N. Jenkins. Control of multi-terminal VSC-HVDC transmission for offshore wind power. pages 1 –10, sept. 2009.

[8] L. Xu and L. Yao. DC voltage control and power dispatch of a multi-terminal HVDC system for integrating large offshore wind farms. *Renewable Power Generation, IET*, 5(3):223 –233, May 2011.

[9] W. Lu and B.T. Ooi. Optimal acquisition and aggregation of offshore wind power by multiterminal voltage-source HVDC. *IEEE Power Engineering Review*, 22(8):71–72, Aug. 2002.

[10] J. Rudolph and F. Woittennek. Motion planning and open loop control design for linear distributed parameter systems with lumped controls. *International Journal of Control*, 81(3):457–474, 2008.

[11] J. Rudolph. *Flatness Based Control of Distributed Parameter Systems*. Shaker Verlag, 2003.

[12] F. Woittennek. *Beiträge zum Steuerungsentwurf für lineare, örtlich verteilte Systeme mit konzentrierten Stelleingriffen*. Shaker Verlag, 2007.

[13] K. Küpfmüller, W. Mathis, and A. Reibiger. *Theoretische Elektrotechnik*. Springer Verlag, 2006.

[14] M. Fliess, P. Martin, N. Petit, and P. Rouchon. Active signal restoration for the telegraph equation. In *Proc. Conference on Decision and Control*, 1999.